Int. J. Solids Structures Vol. 19, No. 10, pp. 857–872, 1983
Printed in Great Britain.

0020-7683/83 $3.00 + .00

FINITE PLASTIC STRAIN IN ANNEALED MILD STEEL DURING PROPORTIONAL AND NON-PROPORTIONAL LOADING

JAMES F. BELL
Department of Mechanics, The Johns Hopkins University, Baltimore, MD 21218, U.S.A.

(*Received* 29 *July* 1982; *in revised form* 14 *January* 1983)

Abstract—Proportional and non-proportional loading experiments show that the finite strain plastic response of annealed mild steel between the termination of the initial yield and the termination of the ultimate stress closely follows the predictions of an incremental theory of finite plastic strain for which stress and strain components are referred to the original, undeformed reference configuration.

Experimental study of the initial yield domain in terms of dead weight loading of mild steel has shown that the initiation and termination of this region also may be described in terms of the same parabolic generalization.

Finally, for annealed mild steel in dead weight loading, the generalized stress at failure is shown to occur on a common von Mises loading surface.

INTRODUCTION

With reference to constitutive statements for solid mechanics probably the two most studied common metals during the past 150 years are annealed copper and mild steel. In a recent paper in this Journal, an experimental study of the finite plastic strain of the face-centered cubic solid, annealed copper [1], revealed a detailed correlation with a recently developed, incremental theory of finite strain plasticity [2, 3]. Given the long interest in comparing these two metals, it is in order to make an identical study of the body-centered cubic solid, annealed mild steel. In the domain of finite plastic strain, annealed copper and annealed mild steel have markedly different properties, particularly with respect to their material stability in that region of strain and with respect to their elastic limits at its initiation. Thus, while the present paper reports upon identical *measurements*, albeit at stress levels three to four times higher for annealed steel than for annealed copper, the results could by no means be securely predicted at the inception of the experimental series.

All measurements were from dead weight loading at constant stress rates, and included arbitrarily chosen proportional and non-proportional stress paths. The copper specimens had been thin-walled tubes loaded in tension and torsion, also along arbitrarily chosen proportional and non-proportional loading paths. The majority of tests described here were thus conducted on annealed, seamless, 1020 mild steel tubes for a comparison with the copper sequence. For mild steel, however, prior thermal histories play an important role in the inception of finite strain. Therefore, additional tension and compression measurements on variously annealed solid cylinders of mild steel were included.

The incremental theory of the present author, developed from an analysis of experiment on several ordered solids [2, 3], and which now comprehends mild steel, refers all stress and strain components to the original, undeformed reference configuration of the fully annealed solid. So defined, and implicit in the theory, are the effective or generalized stress, the effective or generalized strain, and the characterization of yield and loading surfaces.

EXPERIMENT AND THEORY

In order that this paper shall be self-contained, the present analysis delimits the general theory to its application to the above types of tests. We introduce $\sigma = (\text{axial force}/A_0)$ as the axial stress and $S = (\text{torque}/r_m A_0)$ as the torsional shear stress, where A_0 is the original undeformed cross-sectional area, and r_m is the original mean radius of the thin-walled tube. The axial strain is given as $\epsilon = (l - l_0/l_0)$ and the torsional shear strain as $s = (r_m\theta/l_0)$, where l_0 is the original undeformed length; l is the deformed length; and θ, in radians is the measured angle of twist. In these terms, if a generalized scalar measure of stress, T, is defined by eqn (1)

$$T = \sqrt{\left(\frac{2}{3}\sigma^2 + 2S^2\right)} \tag{1}$$

and a generalized measure of strain, Γ, is defined in incremental form by eqn (2)

$$d\Gamma = \sqrt{\left(\frac{3}{2}(d\epsilon)^2 + \frac{1}{2}(ds)^2\right)}, \tag{2}$$

then literally hundreds of tests on 30 different fully annealed crystalline solids (including relatively pure annealed metals of 5 different crystal structures and two non-metals, rock salt and semi-crystalline nylon†) led to the purely experimental discovery that during the large finite strain deformation of these ordered solids the generalized stress and strain are related parabolically by eqn (3)

$$d\Gamma = \frac{2T\,dT}{\beta^2} \tag{3}$$

where β is a measured constant.

For proportional or radial loading histories in which the ratios of stresses remain constant while the strain components continue to large finite deformation, the generalized strain Γ through integration is given by eqn (4)

$$\Gamma = \sqrt{\left(\frac{3}{2}\epsilon^2 + \frac{1}{2}s^2\right)}; \tag{4}$$

or, in terms of the orthogonal strain components ϵ_i, referred to the undeformed reference configuration we have eqn (5)

$$\Gamma = \sqrt{(\epsilon_1^2 + \epsilon_2^2 + \epsilon_3^2)}. \tag{5}$$

Whereas proportional loading tests demonstrating the applicability of eqn (3) have been performed on 50 solids, including structural metal alloys, the non-proportional stress histories of 12 of the 50 crystalline solids have been considered thus far. From non-proportionnal loading tests, particularly those which include sharp directional changes in loading path, we see that not only is the parabolicity of eqn (3) applicable but also the generalized strain Γ in every instance is stress path dependent, and the description of the deformation requires the introduction of incremental constitutive statements.

Although the choice of stress definition and strain measure is arbitrary, usually based upon the effort to achieve analytical simplicity, for the finite strain of the 50 solids examined during loading, i.e. when $dT \geqslant 0$, experiment alone reveals that one may simplify as well as unify the description of finite deformation plasticity when the stress and the strain components are all referred to the undeformed configuration of the solid. Analysis of experiment, with loading stress paths in various combinations of axial loading and torsion, provides the constitutive statements of eqns (6) and (7).

$$d\epsilon = \frac{4\sigma\,dT}{3\beta^2} \tag{6}$$

$$ds = \frac{4S\,dT}{\beta^2}, \tag{7}$$

where

$$dT = \frac{\frac{2}{3}\sigma\,d\sigma + 2S\,dS}{T}$$

Equation (3) is applicable for both proportional and non-proportional loading paths. For

†The experiments on nylon-6 were performed at the Indian Institute of Technology, Delhi, by Indu Prakash Singh.

proportional loading, eqns (6) and (7) readily may be integrated, providing eqns (8) and (9).

$$\epsilon = \frac{2\sigma T}{3\beta^2} + \epsilon_b \tag{8}$$

$$s = \frac{2ST}{\beta^2} + s_b \tag{9}$$

Equations (1)–(9) are given here as a set of relations describing and unifying extensive experimental observation. In eqns (6)–(9) the value of the constant, β, is measured and plays a role in parabolic plasticity similar to that of the elastic constants in linear elasticity.

For a number of crystalline solids such as annealed high purity copper, high purity aluminum, depleted uranium, etc. a single constant, β, for each solid may apply throughout the finite strain plastic domain to strain components in excess of 30%. For a number of other crystalline solids such as the 1020 annealed mild steel of interest here, low purity aluminum, low purity zinc, etc., a particular value of the constant β may be associated with one large segment of finite strain, and a shift to a different constant value may be associated with an adjacent large segment of finite strain.

It has been shown [1] that the present writer's incremental theory of parabolic plasticity applies to the finite deformation of a member of the first group, high purity annealed copper. The present paper provides evidence that this same incremental theory of plasticity [2, 3] applies to a crystalline solid, annealed mild steel, illustrative of the second group, with a high density, second-order transition structure.

The behavior when second-order transitions are absent is illustrated in Figs. 1 and 2 from

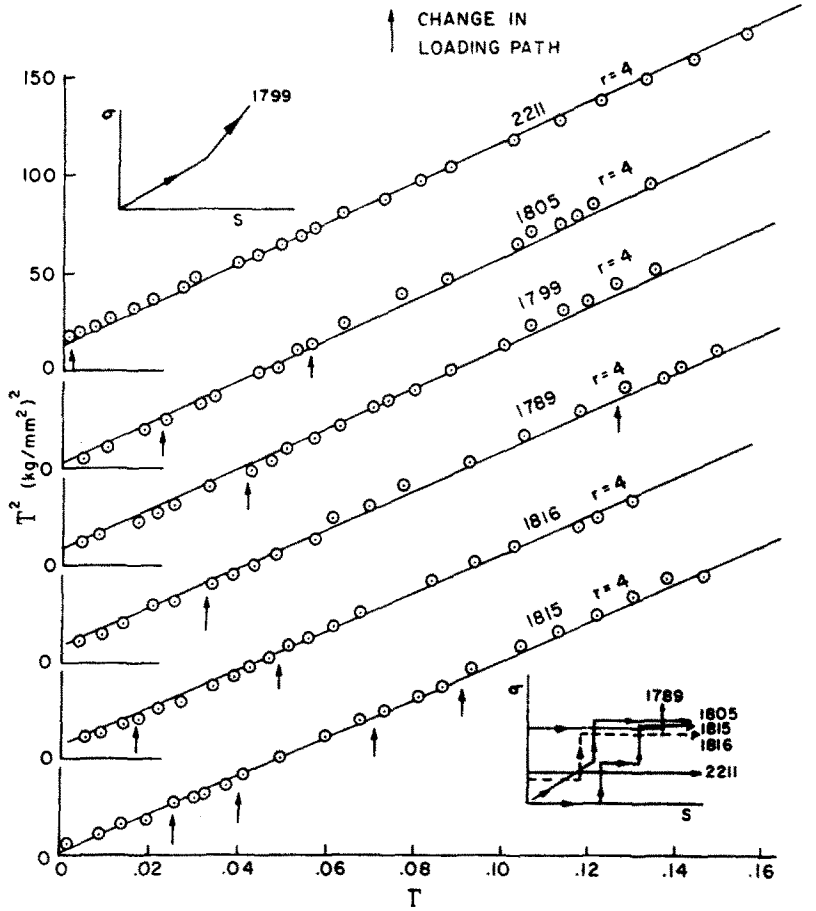

Fig. 1. Theory, eqn (3), (solid lines) vs experiment (circles) from the measurements of Bell and Khan [1] on transition free annealed copper for the non-proportional tension–torsion paths shown. $\beta = 37.0$ kg/mm^2.

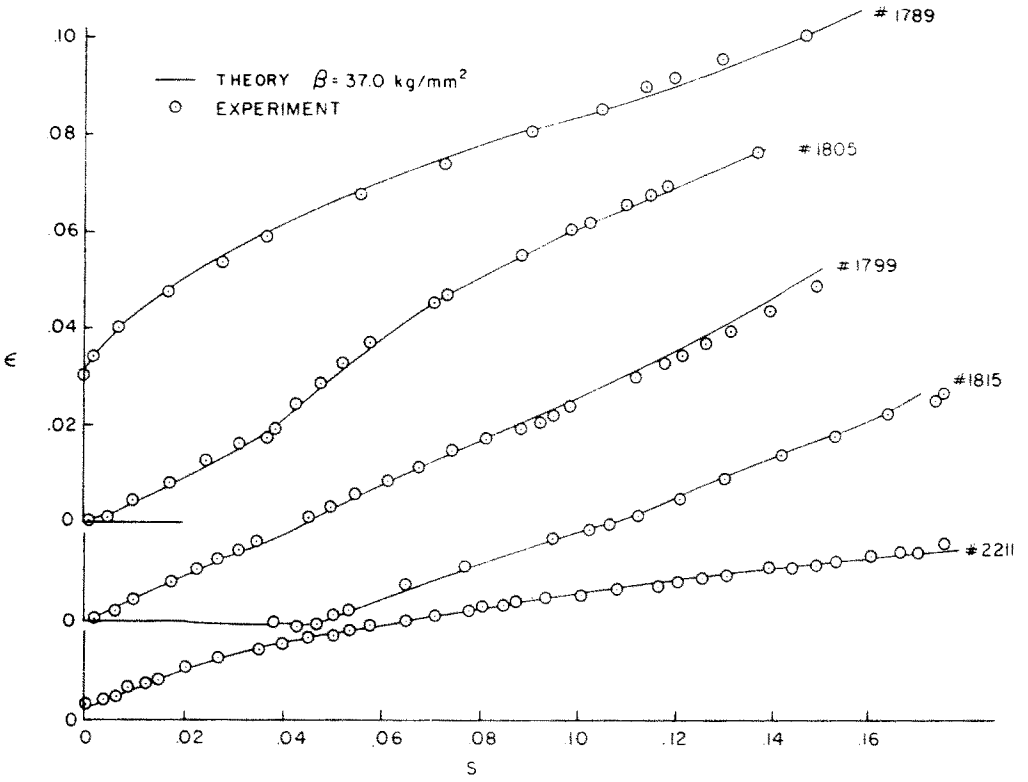

Fig. 2. The integration of eqns (6) and (7) (theory) compared with measurement on annealed copper (circles) from the experiments of Bell and Khan [1].

the paper [1] on high purity annealed copper. In Fig. 1 the parabolicity of eqn (3) is evident in the T^2 vs Γ plots for the variety of non-proportional stress paths considered.

As may be seen in Fig. 1, the value of the constant parabola coefficient, $\beta = 37.0\,\text{kg/mm}^2$, is the same for all stress paths, i.e. from experiment we see that in this solid a common value of β governs the finite strain domain in terms of generalized stress, T, and generalized strain, Γ, for $dT \geq 0$.

In Fig. 2, from that same paper [1], we see the close correlation between theory (solid line) and experiment (circles) in ϵ vs s strain space. The solid lines were determined from the integration of eqns (6) and (7) for the stress paths indicated in Fig. 1.

The same type of experiments on annealed mild steel provides the T^2 vs Γ plot shown in Fig. 3. The tension-torsion, dead weight loading apparatus was that used in the copper study [1].

For solids with a high density second-order transition structure such as that shown in Fig. 3 for annealed 1020 steel, a T^2 vs Γ plot gives a series of straight line segments indicating parabolicity, with different values of the constant β in the different finite deformation domains. Such a transition structure for simple loading, that is, for a single stress component, has been described in a series of papers beginning in 1964: e.g. [4–7]; in a summary for 27 crystalline solids in a monograph in 1968 [8]; and, in great experimental detail, in a *Handbuch der Physik* treatise in 1973 [9].

The experiments with two or more non-zero stress components reveal that such transitions appear in the structure of the response function for the generalized stress and generalized strain. As with simple loading for which long tabulations already have been provided, the location of the observed discontinuities is not arbitrary. When a transition occurs, its location is representable by one of eight known strains which from the statistical analysis of hundreds of tests can be categorized by eqn (10).

$$\Gamma_N = \frac{1}{\sqrt{2}}\left(\frac{2}{3}\right)^{N/2} \tag{10}$$

where $N = 0, 2, 4, 6, 8, 10, 13, 18$.

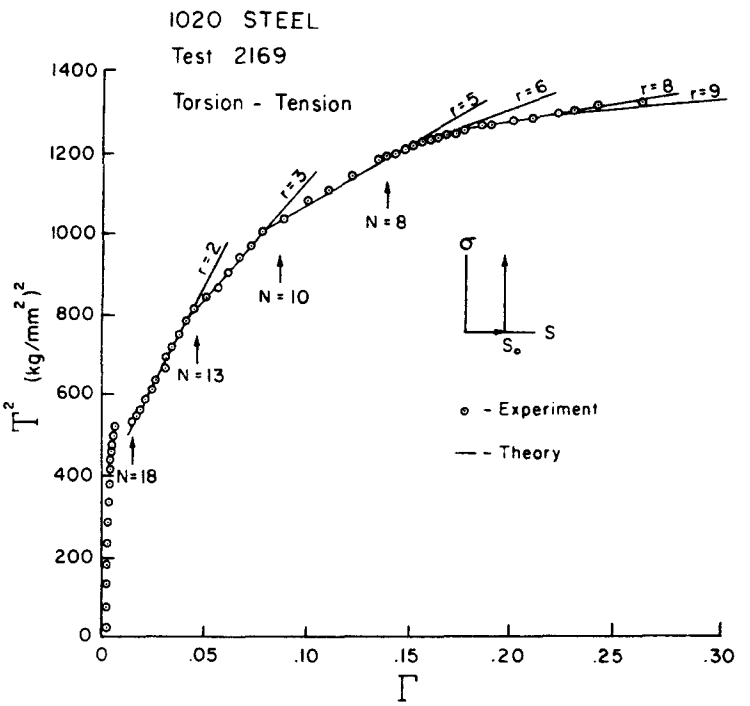

Fig. 3. A typical non-proportional measurement on high transition density mild steel, compared with prediction, eqn (3).

When we compare Figs. 3 and 1, we see that annealed mild steel, unlike annealed high purity copper, has a high density second-order transition structure, yet eqn (3) with its concomitant parabolicity still is applicable for any given domain or deformation mode.

Next we ask: do the constitutive statements of eqns (6) and (7), known to apply to nearly transition-free annealed copper and high purity aluminum during both proportional and non-proportional loading, also apply when the response function is multi-structured? To determine whether this be so, a series of experiments on thin-walled tubes of annealed mild steel were performed. This series of experiments were for the proportional and non-proportional loading paths in axial tension and torsion, as shown in Fig. 4.

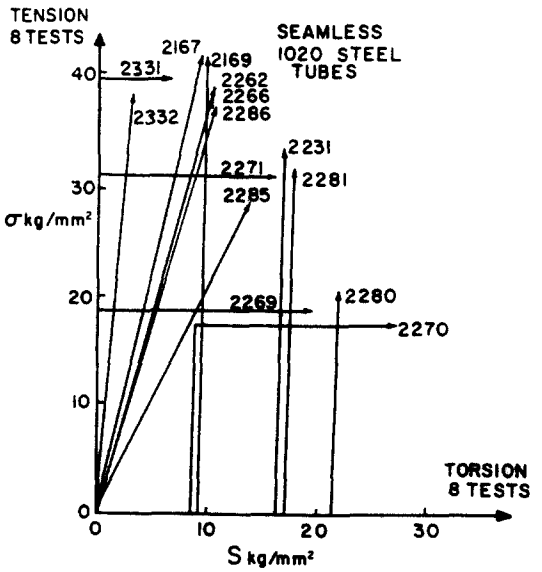

Fig. 4. Proportional and non-proportional loading paths for 30 tests on annealed mild steel.

All of those tests provide T vs Γ segmented parabolicity of the type shown in Fig. 3 for test No. 2169. The location of the arrows for the stated values of N in Fig. 3 are from the averages for several hundred tests in a number of solids [8, 9]. Test 2169 was for a non-proportional loading path in which initial simple torsion was followed by axial tensile loading at constant shear stress. It characterizes the common relation between the generalized shear stress and the generalized shear strain for all loading paths examined, whether proportional or non-proportional.

The applicable value of the constant β being known from T^2 vs Γ plots, the integration of eqns (6) and (7) over the successive segments provided the close correlation between the incremental theory, eqns (3), (6) and (7) [solid lines] and experiment [circles] in ϵ vs s strain space, as in Fig. 5.

Thus, from these experiments on the finite strain of mild steel we see that this incremental theory, with stress and strain components referred to the undeformed reference configuration. remains applicable when second-order transitions are present.

In this Journal in 1978, Tate [10] proposed a new approach to the theory of plastic deformation, one which encompasses the present writer's finite deformation mode and transition structure. As in the present study, stress and strain for a parabolic response function with the parabola coefficient of eqn (11) below are given with respect to the undeformed configuration. Tate assumed that the transition phenomenon arises from the interplay of plastic deformation mechanisms on different structures. Subsequent experiment (see Section 7, pp. 115–117 of Ref. [3]) has indicated that at least for mild steel there is need for a modification of the role of the linear elastic component from that assumed in Tate's theory. This should not offer serious difficulty to the continued development of plasticity theory which includes the observed transition phenomenon.

Like the critical strains of eqn (10), from which are calculated the four locations shown in Fig. 3, the magnitude of the sequence of slopes shown in the same figure are not arbitrary. They arise in the finite strain deformation mode and transition structure (see Ref. [2, 3, 5–8] and Chap. IV of Ref. [9].) This quantum structure, difficult to observe when the strain history is specified in a "hard" testing machine, particularly when data are plotted in the traditional terms of Cauchy or "true" stress and logarithmic or "true" strain, is readily observable when one

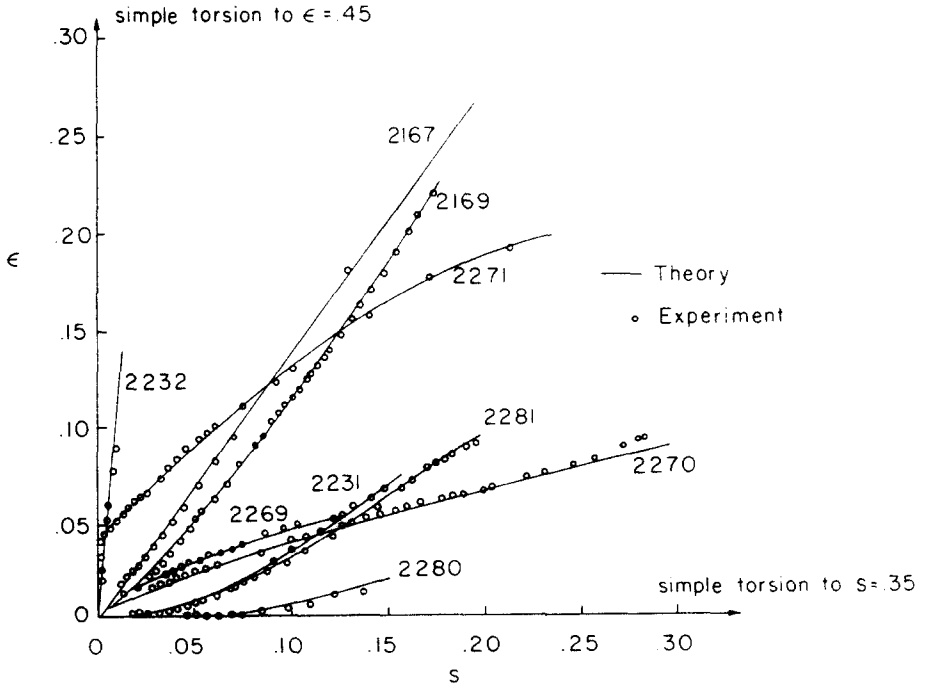

Fig. 5. A comparison of the integration of eqns (6) and (7) (solid lines) with measurements (circles) for high transition density annealed mild steel.

considers dead weight loading for data in a stress squared vs strain plot, with a stress and strain referred to the undeformed configuration.

The essence of this experimental discovery, which required two decades and many hundreds of experiments to document, is that the numerical values of the slopes, the constant β, are not found in an empirically arbitrary form but have a quantized structure. For 50 ordered solids of 7 different crystal structures, the value of β is given by eqn (11), where μ (0) is the elastic shear modulus in the vicinity of absolute zero temperature; T is the ambient temperature of the test; T_m is the melting point of the solid of interest; $B_0 = 0.0207$ is a dimensionless universal constant for all ordered solids studied; and $r = 1, 2, 3, 4\ldots$ is the integral mode index of the finite deformation mode structure.

$$\beta = \left(\frac{2}{3}\right)^{r/2} \mu(0) B_0 (1 - T/T_m). \tag{11}$$

For mild steel (see Appendix 2 of Ref. [8], or Table 107, p. 398 of Ref. [9]), $\mu(0) = 8580\ \text{kg/mm}^2$, $T_m = 1809°\text{K}$, so that for a room temperature of $T = 294°\text{K}$, the values of β for the indicated values of r are shown in Table 1. For annealed copper with $\mu(0) = 5080\ \text{kg/mm}^2$ and $T_m = 1356°\text{K}$, the almost universally observed value for $r = 4$ at room temperature provides $\beta = 37.0\ \text{kg/mm}^2$ calculated from eqn(11) and correlates with the observed values in Fig. 1.

The experimental study of finite deformation in several metals subjected to non-proportional loading paths has made evident that Γ is path dependent. As a consequence of this observation, the response had to be described in incremental form. For non-proportional loading paths in which either the axial stress σ or the shear stress S are constant, i.e. σ_0 or S_0, either eqn (6) becomes eqn (12) or eqn (7) becomes eqn (13), depending upon which stress component is constant.

$$\frac{dT}{d\epsilon} = \frac{3\beta^2}{4\sigma_0} = \text{constant} \tag{12}$$

$$\frac{dT}{ds}\frac{\beta^2}{4S_0} = \text{constant}. \tag{13}$$

The observation of linearity in either a T vs ϵ or a T vs s plot establishes the applicability of the incremental theory of eqns (3), (6) and (7). With the magnitude of the constant stress known, either σ_0 or S_0 as the case may be, the measured value of the slope provides the value of the parabola coefficient β. In every instance the values so obtained were those of Table 1.

ON THE INITIAL YIELDING OF MILD STEEL

Historically, the behavior of mild steel at the small strain of the yield point has been variously interpreted. In the second half of the 20th century, "hard" testing machines in which

Table 1.

	$T = 294°\text{K}$	
	β	
$r = 0$	148.74 kg/mm^2	21.16 x 10^4 psi
$r = 1$	121.45 kg/mm^2	17.27 x 10^4 psi
$r = 2$	99.16 kg/mm^2	14.10 x 10^4 psi
$r = 3$	80.96 kg/mm^2	11.52 x 10^4 psi
$r = 4$	66.11 kg/mm^2	9.40 x 10^4 psi
$r = 5$	53.98 kg/mm^2	7.68 x 10^4 psi
$r = 6$	44.07 kg/mm^2	6.27 x 10^4 psi
$r = 7$	35.98 kg/mm^2	5.12 x 10^4 psi
$r = 8$	29.38 kg/mm^2	4.18 x 10^4 psi

the strains are imposed and the stresses are the measured unknowns, are in almost universal use, and the anomolous initial yielding of mild steel appears in the much studied form of the double yield limit. In the 19th and early 20th centuries, dead weight loading was the dominant method of mechanical testing, i.e. the stress components are imposed and the strain components are the unknown quantities to be measured. In this latter type of test the initial yield occurs not as double yield but as a jump in strain at constant or nearly constant stress.†

The appearance of this constant stress plateau at the elastic limit is a rarity among solids, and, at room temperature, mild steel is the only exception among the commonly studied metals. Nevertheless, the importance of mild steel in practical technology, the concentration of engineering theories of plasticity on small strain, and the volume of the earlier literature on steel (measurements on this solid alone were comparable to the combined total on all other metals) provided an illusion of generality for what was, in fact, a special case.

The observed behavior in dead weight loading is shown in the T vs Γ plots of Fig. 6(a) for seven simple torsion tests on seamless, thin-walled tubes of 1020 steel. The circles designate the measured data. The magnitude of the constant stress rate changes from one test to another. In every instance we see that the end of initial yield occurs at the first transition strain of eqn (10), $\Gamma_{N=18} = 0.01837$.

For 26 tests for seamless 1020 steel tubes in simple torsion, simple tension, radial loading, and non-proportional loading, the average measured value of Γ at the end of the initial yield is

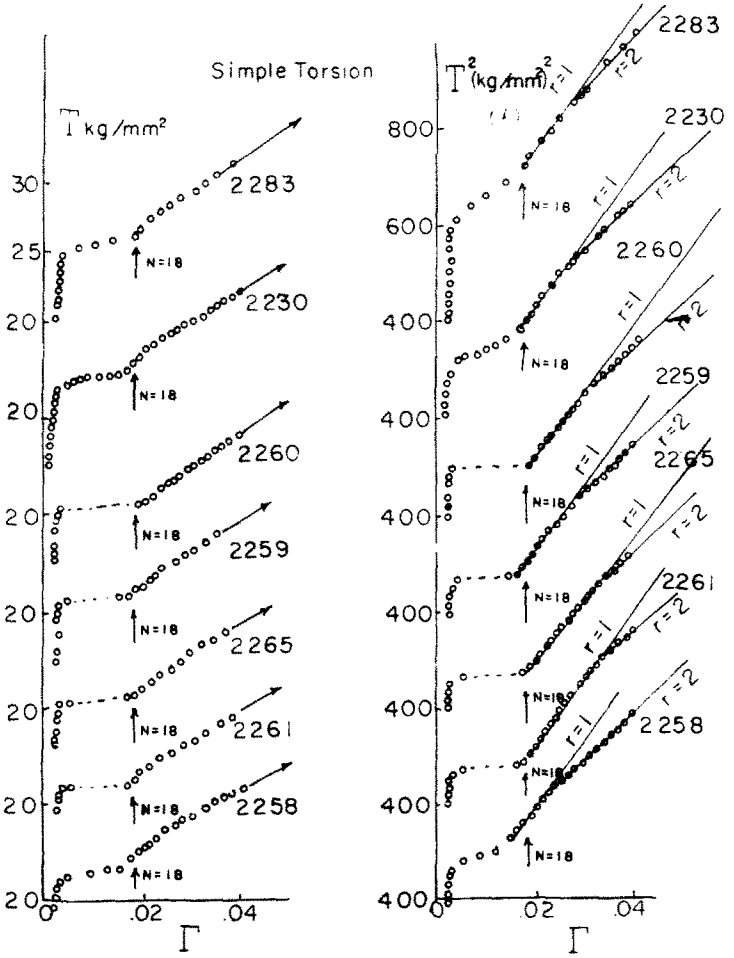

Fig. 6. T vs Γ (a) and T^2 vs Γ (b) for the initial yield of 7 simple torsion tests in dead weight loading, showing the termination at $\Gamma_{N=18}$.

†The identical situation is found for the Savart-Masson (Portevin-le Chatelier) effect. The "hard" testing machines provide oscillations, whereas in dead weight loading one has the staircase phenomenon or a series of small, constant stress plateaus.

$\Gamma = 0.0183 \pm 0.0004$, or $\Gamma_{N=18}$ of eqn (10). The determination of these values of Γ was made from T^2 vs Γ plots such as those of Fig. 6(b). The end of initial yield was identified as the beginning of parabolicity, which usually has the deformation mode of $r = 1$ in eqn (11) or Table 1. The subsequent finite strain behavior was the subject of the previous sections of this paper.

This type of initial yield in dead weight loading of annealed 1020 mild steel is not confined to simple torsion, as may be seen in the T vs Γ plots of Fig. 7. Figure 7(a) shows the initial portion of a representative series of proportional or radial tests (i.e. simultaneous twisting and pulling) with the constant stress ratios $\dot{\sigma}/\dot{S}$ indicated. Figure 7(b) is representative of non-proportional tests for which one type of loading is followed by the other, as indicated. One load is held constant while the other increases at a designated constant stress rate, and vice versa. The 90° corner from tension to torsion, or from torsion to tension was variously located during the deformation, even being located in the interval of initial yield. This had no visible effect upon the response.

In Fig. 7(c) are shown two of the several tension tests, and in Fig. 7(d) two of the compression tests which exhibited the characteristic initial yield to $\Gamma_{N=18}$.

In the series of 30 tests on thin-walled, seamless 1020 steel tubes, four tension tests provided the common elastic limit $T_Y = 20.93\ \text{kg/mm}^2$ but began with parabolicity immediately, without exhibiting the initial yield behavior. This is the type of response characteristic of all of the other 49 solids in which finite strain has been studied. Of the total of 44 tests on mild steel discussed in the present paper, these four are the only tests which failed to provide the characteristic initial yield for dead weight loading.

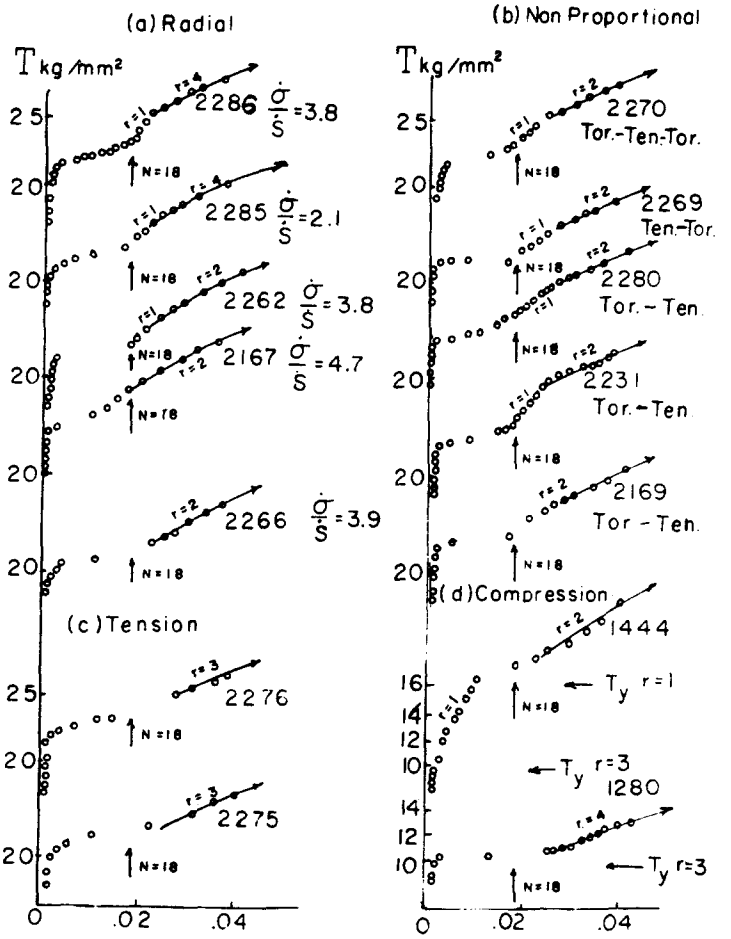

Fig. 7. T vs Γ plots for the initial yield region for (a) radial, (b) non-proportional, (c) tension, and (d) compression tests on mild steel, showing that the termination of the initial yield region at $\Gamma_{N=18}$ is loading path independent.

For the 30 annealed, seamless thin-walled tubes of 1020 steel, the average T_Y is $T_Y = 20.93 \pm 0.16\ kg/mm^2$ (29,770 ± 226 psi). To independently vary the load at T_Y and thus provide a further check upon the minimal effects of friction, 18 of the tests in this series were for specimens with an outside diameter of 10.541 mm (0.4150 in.) and 12 were for an outside diameter of 11.176 mm (0.4400 in.). For both groups the inside diameter was 9.525 mm (0.3750 in.), providing wall thicknesses of 0.508 mm (0.0200 in.) and 0.826 mm (0.0325 in.), respectively. Since the area of each group of specimens is different, the elastic limit occurs at different values of the applied load. Hence, the obtaining of equal values of the stress, T_Y, provides a check that the measured value is independent of apparatus. The ratio of loads at T_Y and elsewhere for the two groups is 1.676 for the tension component and 1.729 for the shear component. The average T_Y for the 18 smaller outside diameter tubes is $T_Y = 20.92 \pm 0.23\ kg/mm^2$. For the 12 large outside diameter tubes, $T_Y = 20.95 \pm 0.21\ kg/mm^2$. All this attests to the fact that the effort to reduce friction in the apparatus to negligible levels has been successful, as other independent checks had indicated during the modification of the apparatus for the higher stresses required for studies of steel.

Before commenting further upon the fact that the initial yield begins at a common T_Y and ends at a common transition strain $\Gamma_{N=18}$ in the above series of tests, we shall consider the effects of varying prior annealing conditions for the same type of 1018 or 1020 mild steel.

The tests performed in either tension or compression on solid steel cylinders, included: specimens from "as received" hot rolled 1020 steel rod; specimens annealed for one hour at 649°C (1200°F) immersed in carbon; specimens annealed for 0.5 hr at 927°C (1700°F) in a vacuum; and specimens annealed in a vacuum at 893°C (1640°F) for 24 hr or for 48 hr.

All 14 of these tests, whether in tension or compression, exhibited the same form of initial yield in dead weight testing as that for seamless steel tubes shown in Figs. 6 and 7. The value of the yield limit T_Y, however, was lowered in a uniform manner as a result of the altered prior thermal history.

These dead weight tests were for prescribed incremental loading. A beam in constant balance applied the load in either tension or compression. Two compression tests on "as received" hot rolled 1020 solid steel specimens, shown in Fig. 8, exhibit the degree of reproducibility obtainable under identical conditions. The initial yield region ends at $\Gamma_{N=18} =$

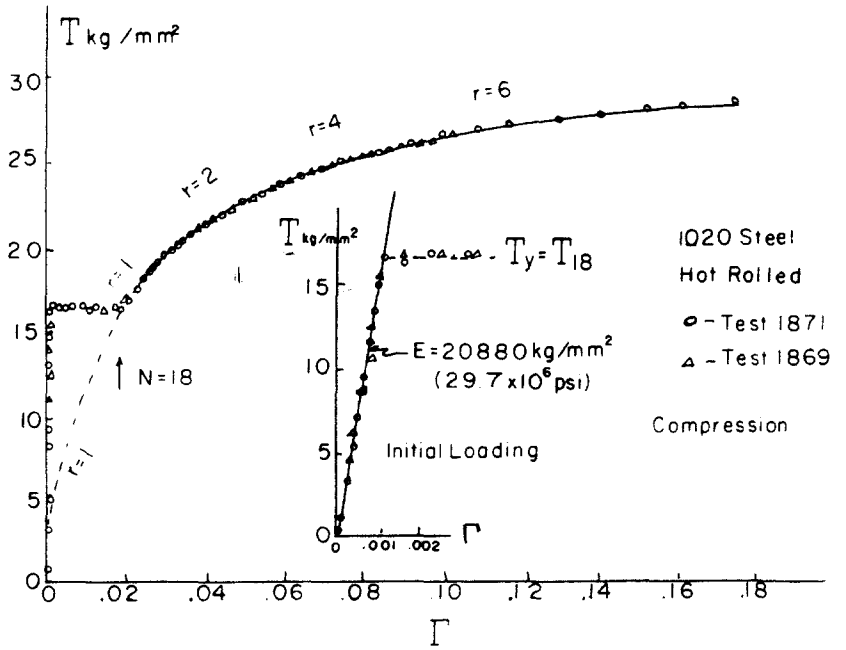

Fig. 8. T vs Γ for two compression tests on hot rolled 1020 steel, showing the initial yield region terminating at $\Gamma_{N=18}$ on an $r = 1$ parabola from the origin. The insert provides the detail of the small strain at the yield limit.

0.0184 as in the tests described above, but the initial yield stress is reduced to T_Y = 16.65 kg/mm^2 (23,682 psi) from the value of 20.93 kg/mm^2 for the seamless steel tubes. T^2 vs Γ data (not shown) make apparent that the finite strain for $\Gamma \geqslant \Gamma_{N=18}$ is in accord with the finite strain theory described above in eqns (3), (6) and (7) for the indicated finite deformation modes, r, of eqn (11).

Also shown, as an insert in Fig. 8, is the initial deformation for these two tests. We can see in the linear region the correlation with the standard E modulus of 20,880 kg/mm^2 (29.7×10^6 psi). This is followed by a sharp entry into the constant stress, initial yield region. (For T vs Γ the slope is $(2/3)E$ since $T = \sqrt{(2/3)}\,\sigma$ and $\Gamma = \sqrt{(3/2)}\epsilon$ for axial loading.)

Two tests, one in tension (No. 2301) and one in compression (No. 2304) on specimens which were annealed in a vacuum for 0.5 hr at 927°C (1700°F) are shown in the T^2 vs Γ plots of Fig. 9.

Again, the initial yield region terminates at $\Gamma_{N=18}$. It is followed by the parabolicity of the finite strain theory (solid lines) for the indicated deformation modes, r. The initial yield stress T_Y is approximately the same as that for the "hot rolled" rod of Fig. 8, i.e. T_Y = 16.66 kg/mm^2 (23,700 psi) for test 2301 and T_Y = 17.52 kg/mm^2 (24,917 psi) for test 2304. The tensile specimen has an 101.6 mm (4 in.) test section and a 12.7 mm (0.5 in) diameter, while the compression specimen lubricated at the ends has a 25.4 mm (1 in.) diameter and an L/D ratio of 3, which required that the test be performed with great care, using lubricated spherical seats.

Compression tests 1244, 1250, 1251 and 1252, for specimens annealed in carbon for 1 hr at 649°C (1200°F) and cooled in the furnace for 24 hr, exhibited the same behavior at initial yield and finite strain as those of Figs. 8 and 9, with the same lower value of T_Y.

For 10 other specimens in this variously annealed group, some were annealed in a vacuum for 24 hr at 893°C (1640°F) and others were annealed in a vacuum for 48 hr at that same temperature. Both sets of specimens were cooled in the furnace. The results obtained from all tests are summarized in Table 2.

In sum, four values of T_Y have been observed: $T_Y = 20.93 \pm 0.16$ kg/mm^2 for 30 tests in the proportional and non-proportional loading of 30 seamless steel tubes; $T_Y = 16.48 \pm 0.19$ kg/mm^2

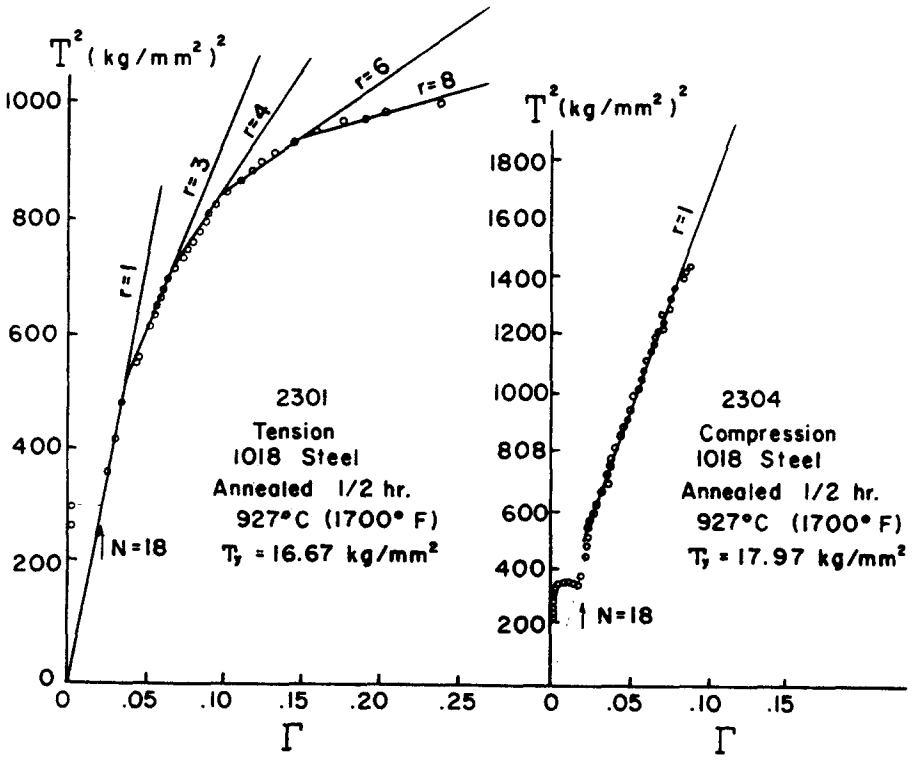

Fig. 9. The T^2 vs Γ plots of tension and compression specimens machined from 1018 steel bar stock, both specimens then annealed 0.5 hr at 927°C (1700°F) and furnace cooled.

Table 2.

r	Calculated $T_{N=18}$ from equation (14)	Experimental T_Y	No. of tests
0	20.13 kg/mm^2	20.93 ± .16 kg/mm^2	30
1	16.44 kg/mm^2	16.48 ± .19 kg/mm^2	10
3	10.96 kg/mm^2	10.71 kg/mm^2	2
4	8.95 kg/mm^2	8.83 kg/mm^2	2

for 10 axial tests in variously annealed specimens noted above; $T_Y = 10.71$ kg/mm^2 for two tests with long vacuum anneals; and $T_Y = 8.83$ kg/mm^2, also for two tests with long vacuum anneals.

The most interesting discovery in these experiments, aside from the observation that the above incremental theory of finite strain applies for stresses and strains given in terms of the undeformed reference configuration, is the fact that the initial yield limit, T_Y, for annealed mild steel also is expressible in terms of the quantized transition structure and parabolicity implicit in the same theory.

For parabolic deformation [i.e. the finite strain theory of eqns (3), (6) and (7)], with the origin of the parabola coincident with the origin at zero stress and zero strain, and with the parabola coefficients of eqn (11), we have eqn (14).

$$T_{N=18} = \left(\frac{2}{3}\right)^{r/2} \mu(0) B_0 (1 - T/T_m)(\Gamma_{N=18})^{1/2}. \tag{14}$$

For $\Gamma_{N=18} = 0.01837$, and with $\mu(0)$, B_0, T, and T_m known, as indicated for eqn (11) above, we may determine the values of $T_{N=18}$ for different integral mode indices, r. For $r = 0$, $T_{N=18} = 20.13$ kg/mm^2; for $r = 1$, $T_{N=18} = 16.44$ kg/mm^2; for $r = 3$, $T_{N=18} = 10.96$ kg/mm^2; and for $r = 4$, $T_{N=18} = 8.95$ kg/mm^2. The correlation between these calculated values of T_Y and the experimental values for the various prior thermal histories are compared in Table 2.

For the dead weight loading of annealed mild steel these tests reveal that when the stress in the linear elastic domain reaches a value T_Y the elastic response becomes unstable and the deformation proceeds at nearly constant stress until the plastic strain reaches the first transition strain, $\Gamma_{N=18} = 0.0184$. That the elastic limit T_Y is equal to $T_{N=18}$ of eqn (14) for a specific mode index r, as found in these experiments, discloses a previously not suspected relation between linear elastic and parabolic plastic domains. This interrelation of T_Y and $T_{N=18}$ at $\Gamma_{N=18}$ is illustrated in Fig. 8. After the first transition strain, $\Gamma_{N=18}$, the deformation is totally plastic and is described by the incremental theory of finite strain plasticity, eqns (3), (6) and (7).

A summary of the experimental results are shown in the T vs Γ plots of Fig. 10(a), and the corresponding T^2 vs Γ plots of Fig. 10(b).

The values of the yield limit T_Y are expressible, in terms of the finite strain parabolicity, by eqn (15), i.e. $T_Y = T_{N=18}$.

$$T_Y = \left(\frac{2}{3}\right)^{r/2} \mu(0)\, B_0 (1 - T/T_m)(\Gamma_{N=18})^{1/2}. \tag{15}$$

To consider the question as to whether the response function for the non-parabolic plateau for $\Gamma < \Gamma_{N=18}$ depends upon stress velocity and/or strain velocity, tests were performed in the initial yield domain, which provided measured strain rates ranging from 10^{-5} per second to 10^{-3} per second. The results for five such measurements on seamless 1020 steel tubes are shown in Fig. 11.

The applied stress rates, observed strain rates, times to reach $\Gamma_{N=18}$ from Γ_Y at the elastic limit, the total time to reach a strain of 0.053 from Γ_Y, and, finally, the total duration of tests, are all given in Table 3.

Despite the fact that it required 18 min to cross the initial yield region for test 2331, 3 min

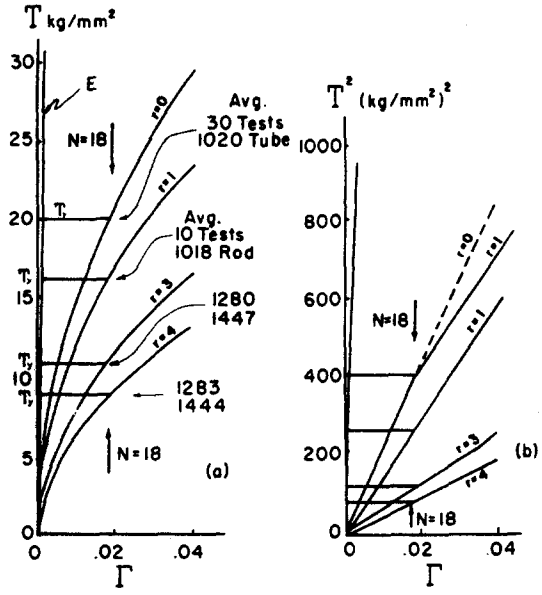

Fig. 10. Schematic diagrams for T vs Γ and for T^2 vs Γ response for the averaged data, showing the different values of T_Y and the corresponding initial parabolas from the origin to $\Gamma_{N=18}$ at the termination of the initial yield region.

for test 2284, and only 2 min for test 2332, the response functions throughout the initial yield domain are identical.

For "hard" testing machines, of course, the strain rate is an arbitrary input. For dead weight loading, of interest here, to produce strain rates higher than 10^{-4} per second, a weight was carefully added in order to load specimen 2330 to a stress 18.54 kg/mm^2 just below T_Y = 21 kg/mm^2, as shown in Fig. 11. A second weight then was carefully added to produce a stress of 27.81 kg/mm^2 for an anticipated strain of approximately 0.05, based on the constant stress rate tests shown. The strain was recorded during loading by means of clip gages. From Γ_Y, the time to reach a strain of 0.053 was 50 sec, compared to 67 min for test 2331; yet for test 2330 the observed strain is that on the $r = 2$ parabola of the slower strain rate measurements.

That a test for which the total loading time is 3 min provides a correlation of response function with one taking a total time of 3 hr and 10 min, suggests a response function for the initial yield region independent of stress and strain velocities.

The critical strain of $\Gamma_{N=18} = 0.01837$ which terminates the initial yield domain was first reported in 1961, as a critical strain in symmetrical free flight impacts of annealed aluminm [11]. For impact velocities producing a maximum strain below that critical strain there was observable near the impact face an initial linear elastic precursor which collapsed into parabolic plasticity at a strain rate $\dot{\epsilon} = 12{,}000\ \text{sec}^{-1}$ after a delay time of from 10 to 20 μ sec. (See, e.g. Figs. 2.33 and 2.34, pp. 42 and 43 of Ref. [8].) For impact velocities producing a maximum strain

Table 3.

Test No.	Avg. $\dot{\Gamma}$ per sec,	$\dot{T}$ kg/mm^2/min.	Time: Γ_Y to $\Gamma_{N=18}$	Time: Γ_Y to $\Gamma_{=.053}$	Total Duration of Test
2276	4.4×10^{-5}	0.485	4 min.	14 min.	63 min.
2284	5.3×10^{-5}	0.759	3 min.	11 min.	40 min.
2332	1.2×10^{-4}	1.031	2 min.	8.5 min.	29 min.
2331	1.3×10^{-5}	0.113	18 min.	67 min.	3 hrs. 10 min.
2330	1×10^{-3}	-----	$\simeq \frac{1}{4}$ min.	50 sec.	3 min.

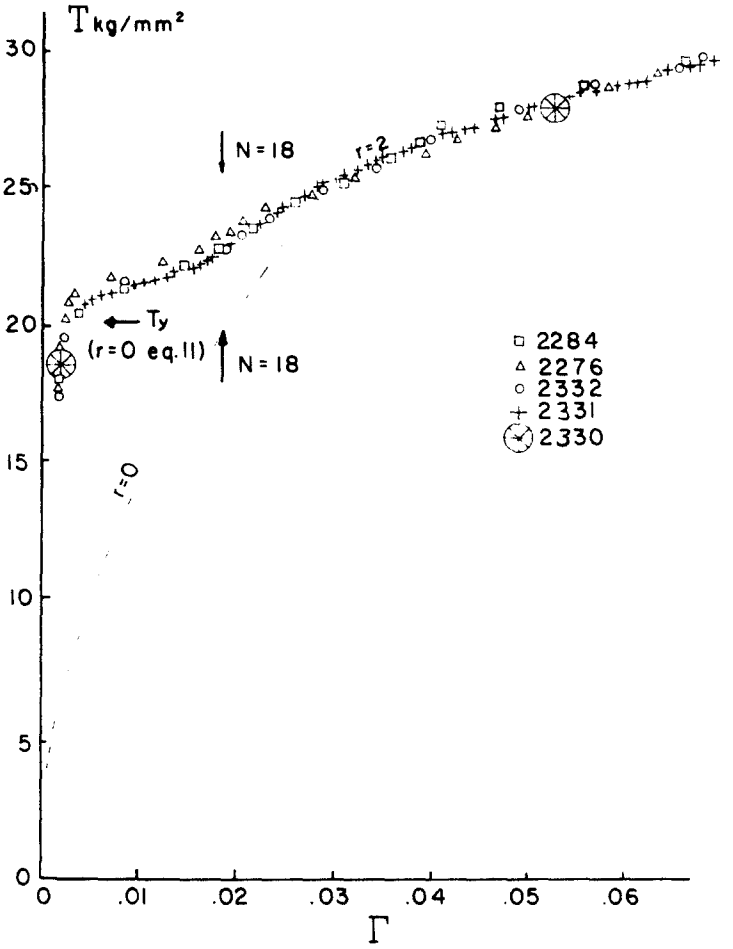

Fig. 11. T vs Γ plots of the results of five dead weight loading tests, showing a common response function for strain rates ranging from 1.3×10^{-5} per sec. for test 2331, to 1×10^{-3} per sec. for test 2330. (See Table 3).

higher than this critical value there is no such delay near the impact face. Such a behavior in the dynamic plasticity of annealed aluminum is consistent with that described here for the quasi-static plasticity of annealed mild steel.

THE ULTIMATE STRESS AND FAILURE OF ANNEALED MILD STEEL IN DEAD WEIGHT LOADING

Three decades ago the form of successive loading surfaces in work hardened solids was an important open question. If, e.g. an initial yield surface were Maxwell–von Mises, would successive surfaces retain the same form? In terms of the experimentally based finite strain theory for parabolic plasticity [2, 3], the answer is a clear "yes", provided stresses and strains are referred to the undeformed configuration. On the other hand, it does not follow that failure should necessarily occur on a common loading surface. That it does so for annealed 1020 mild steel during dead weight loading is therefore a significant additional experimental observation.

Since the Maxwell–von Mises loading surfaces T in σ vs S space are elliptical, it is convenient to transform to circles by the introduction of $\Sigma = \sqrt{(2/3)}\sigma$ and $Q = \sqrt{2}\, S$, so that the generalized scalar measure of stress becomes $T = \sqrt{(\Sigma^2 + Q^2)}$ instead of $T = \sqrt{(2/3)}\,\sqrt{(\sigma^2 + 3S^2)}$.

Twenty-four of the 30 tests on seamless steel tubes described above reached an ultimate stress as evinced in dead weight loading by fracture, pronounced necking in tension, or drastic buckling in torsion. The measured values of T_{ult} are shown in the Σ vs Q plot of Fig. 12. For the 24 tests the average value of T_{ult} is $T_{ult} = 35.41 \pm 0.41$ kg/mm^2 ($50{,}366 \pm 582$ psi). The various loading paths by means of which T_{ult} was reached are shown as dashed lines. (It is interesting

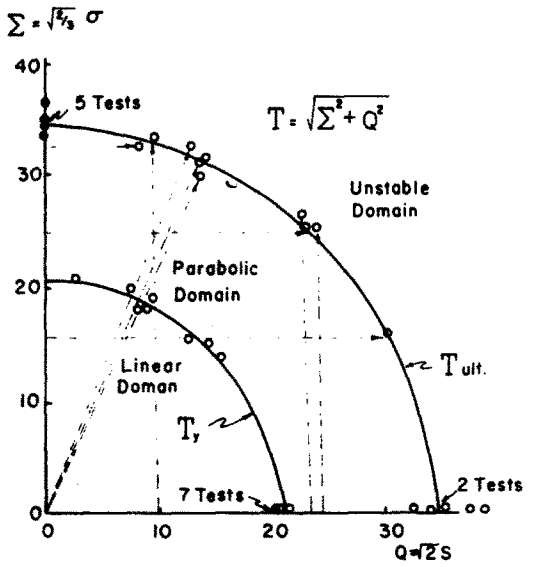

Fig. 12. Maxwell–von Mises loading surfaces for the initial yield, T_Y, and for failure, T_{ult}, for seamless 1020 mild steel tubes. Note that the loading surface at failure is independent of loading path.

that H. E. Tresca in 1868 obtained a value of 37.57 kg/mm^2 as the constant shear flow stress for iron. See Ref. [9], Section 4.4.)

Also included in Fig. 12 are measured values of T_Y for these tests. Both the inner yield surface and the ultimate loading surface are circular in Σ vs Q space and hence are elliptical, or Maxwell–von Mises, in σ vs S space.

Examined by type of test, the total average of $T_{ult} = 35.41$ kg/mm^2 may be compared with the following averages: $T_{ult} = 34.91 \pm 0.42$ kg/mm^2 for 8 tension tests; $T_{ult} = 36.85 \pm 0.91$ kg/mm^2 for 7 torsion tests; $T_{ult} = 34.04 \pm 0.59$ kg/mm^2 for 4 radial tests; and $T_{ult} = 34.77 \pm 0.48$ kg/mm^2 for 5 non-proportional loading tests. Thus the failure criterion for the annealed solid in dead weight loading is sensibly independent of the type of loading, at least in the two dimensional domain.

One also may examine the effect of diametral size on the failure criterion by averaging the data for the two sets of diameters of the 24 tests which underwent failure. Fourteen had an outside diameter of 10.541 mm (0.4150 in.) and an average ultimate stress of $T_{ult} = 34.52 \pm 0.30$ kg/mm^2, while 10 tests with an outside diameter of 11.176 mm (0.4400 in.) provided $T_{ult} = 36.66 \pm 0.74$ kg/mm^2. These, too, may be compared with the total average of $T_{ult} = 35.41 \pm 0.41$ kg/mm^2.

CONCLUSIONS

Despite the anomolous initial yield behavior and high density transition structure, proportional and non-proportional loading experiments have revealed that the finite strain of annealed mild steel is governed by constitutive equations of an incremental theory of finite plastic strain common to the class of ordered solids. Unlike some of the high purity metals such as aluminum and copper at room temperature which have no deformation mode transitions until 20 or 30% strain, annealed 1020 steel, like low purity annealed aluminum for example, undergoes a sequence of transitions from one integral deformation mode to another at nearly every transition strain. The integration of constitutive statements for both proportional and non-proportional arbitrarily chosen loading paths nonetheless provides response functions in strain space in detailed accord with theoretical prediction.

Of equal interest are the results obtained here from dead weight loading in the initial yield region. Depending upon the prior thermal and mechanical histories, the elastic limits T_Y of mild steel are found to be determinable as the calculated stress of a prescribed parabolic deformation mode which passes from the origin at zero T and Γ through the first transition strain at $\Gamma_{N=18}$. The initial linear deformation to the elastic limit T_Y precedes a stress plateau which terminates at the predicted end point, at $\Gamma_{N=18}$ in T vs Γ space. In dead weight loading the initial yield region becomes a domain of constant or near constant stress from a fixed strain at the elastic limit Γ_Y to an equally fixed first critical strain $\Gamma_{N=18}$ of the quantized structure.

This incremental theory of finite strain prescribes a series of parabolas for monotonically increasing loading, i.e. $dT \geq 0$. Each successive loading surface is Maxwell–von Mises. The experimental discovery that for dead weight loading, failure occurs on a particular one of these surfaces, independent of the detail of loading paths, may well be of practical, as well as scientific, interest.

REFERENCES

1. J. F. Bell and A. S. Khan, Finite plastic strain in annealed copper during non-proportional loading. *Int. J. of Solids Structures* **16**, 683 (1980).
2. J. F. Bell, A physical basis for continuum theories of finite strain plasticity—I *Archive Rational Mech. Anal.* **70**, 319 (1979).
3. J. F. Bell, A physical basis for continuum theories of finite strain plasticity—II. *Archive Rational Mech. Anal.* **75**, 103 (1981).
4. J. F. Bell, A generalized large deformation behaviour for face-centered cubic solids—high purity copper. *Phil. Mag.* **10**(103), 107 (1964).
5. J. F. Bell, Generalized large deformation behaviour for face-centered cubic solids: Nickel, aluminum, gold, silver, and lead. *Phil. Mag.* **11**(114), 1135 (1965).
6. J. F. Bell, An experimental study of instability phenomena in the initiation of plastic waves in long rods. *Proc. Symp. on Mech. Behavior of Materials under Dynamic Loads*, San Antonio, Texas, 1967. Springer, New York (1969).
7. J. F. Bell, On experiments revealing the distribution of critical strains in the large deformation of solids. *Rendiconti del Seminario Matematico dell'Università e del Politecnico di Torino*, Italia, **30**, 49 (1971).
8. J. F. Bell, *The Physics of Large Deformation of Crystalline Solids*. Springer Tracts in Natural Philosphy, Vol. 14. Springer-Verlag, Berlin (1968).
9. J. F. Bell, The experimental foundations of solid mechanics. *Handbuch der Physik* Vol. **VIa/1**, pp. 1–813. Springer-Verlag, Berlin (1973).
10. A. Tate, A new approach to the theory of plastic deformation. *Int. J. Solids Structures* **14**, 475 (1978).
11. J. F. Bell, Experimental study of the interrelation between the theory of dislocations in polycrystalline media and finite amplitude wave propagation in solids. *J. Appl. Phys* **32**(10), 1982 (1961).